



# Merging analytic and empirical GEO debris synchronization dynamics

Paul V. Anderson<sup>a</sup>, Darren S. McKnight<sup>b</sup>, Frank Di Pentino<sup>b</sup>, Hanspeter Schaub<sup>a,\*</sup>

<sup>a</sup> University of Colorado, Boulder, USA

<sup>b</sup> Integrity Applications Incorporated, USA

Received 13 January 2016; received in revised form 11 April 2016; accepted 17 May 2016

Available online 26 May 2016

## Abstract

The motion of abandoned satellites near the geostationary (GEO) region has been extensively studied, modeled, and compared to the motion of station-kept, operational satellites, providing insights into the evolution of uncontrolled orbits at GEO. Analytic developments produced a family of curves represented in the ascending node versus inclination space describing the long-term precession of the orbit plane at GEO, and forecasted the clustering of objects at the geopotential wells. However, recent investigations were undertaken to characterize apparent anomalistic behavior of GEO objects and classification of objects into related families. This paper provides a unifying summary of early bottom-up analytical theory with more recent top-down operational observations, highlighting the common linkage between these dimensions of GEO object behavior. This paper also identifies the relevance of these patterns of life tendencies for future operations at and near GEO, and discusses the long-term implications of these patterns of life for space situational awareness activities in this regime.

© 2016 COSPAR. Published by Elsevier Ltd. All rights reserved.

**Keywords:** Space debris; Geosynchronous ring; Conga line motion

## 1. Introduction

Visualizations of the geosynchronous (GEO) debris population from the longitude slot-relative perspective of the Earth-centered, Earth-fixed frame demonstrate that the collective, once-daily motion of this population is similar to a transverse wave circulating around the GEO ring with a period of one sidereal day (McKnight and Di Pentino, 2013). Thus, daily latitude cycles for uncontrolled objects neighboring one another in longitude are not, in general, out-of-phase. Fig. 1 shows the longitude/latitude distribution of the GEO debris population extracted from

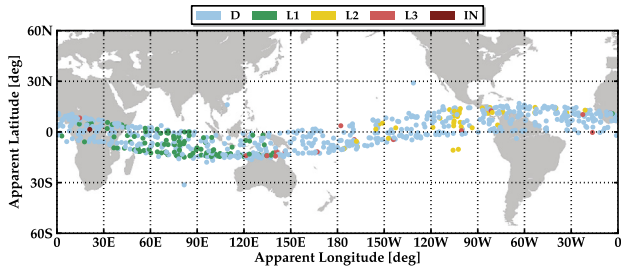
the 28 February 2014 two-line element (TLE) set, at four different times during 01 March 2014, to illustrate this systematic correlation in latitude. As time advances, the peak and trough of this transverse “debris wave” shift westward linearly in longitude. As will be shown in this paper, apparent latitudinal synchronization of the GEO debris population is driven by a combination of inclination and clustering in right ascension of the ascending node (RAAN), the latter resulting from operators leveraging naturally-occurring luni-solar perturbations to reduce north–south station-keeping effort (Capelle and Sharma, 2000).

Upon close inspection of Fig. 1 (and especially if animating the motion of Fig. 1<sup>1</sup>), eight objects in the

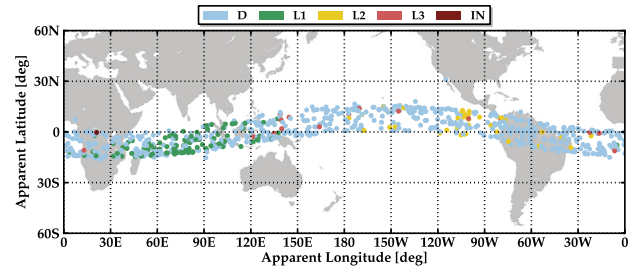
\* Corresponding author.

E-mail addresses: [paul.anderson@colorado.edu](mailto:paul.anderson@colorado.edu) (P.V. Anderson), [dmcknight@integrity-apps.com](mailto:dmcknight@integrity-apps.com) (D.S. McKnight), [fdipentino@integrity-apps.com](mailto:fdipentino@integrity-apps.com) (F. Di Pentino), [Hanspeter.Schaub@colorado.edu](mailto:Hanspeter.Schaub@colorado.edu) (H. Schaub).

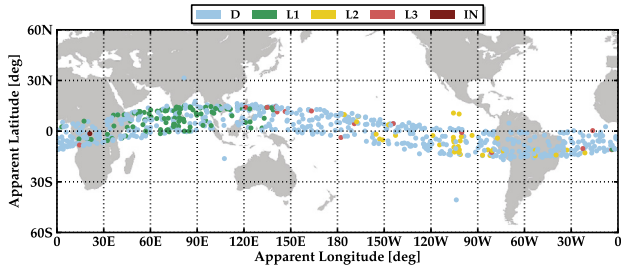
<sup>1</sup> See animation of daily latitudinal motion of derelict GEO population at <http://hanspeterschaub.info/Movies/GeoDebrisConga.mp4>.



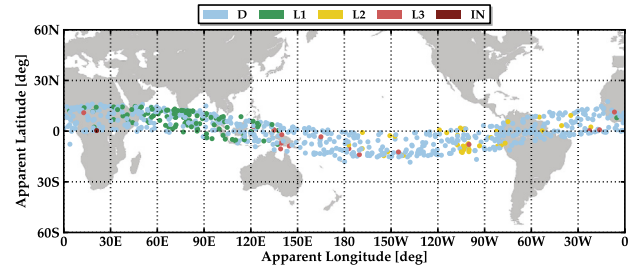
(a) Longitude/latitude distribution of debris population (00:00:00 Zulu).



(b) Longitude/latitude distribution of debris population (06:00:00 Zulu).



(c) Longitude/latitude distribution of debris population (12:00:00 Zulu).



(d) Longitude/latitude distribution of debris population (18:00:00 Zulu).

Fig. 1. Longitude/latitude distribution of the GEO debris population on 01 March 2014, shown in six-hour intervals to illustrate the collective, wave-like behavior of the 745 derelicts comprising this debris population. Objects are colored by uncontrolled orbit class, as listed in Issue 16 of the *Classification of Geosynchronous Objects* report maintained by the European Space Agency (Flohner, 2014).

population qualitatively appear to be either fully or partially unsynchronized with the wave-like latitudinal motion exhibited by the rest of the population. When the local debris populations at or near the longitudes of these outliers are rising in latitude from south to north through the equatorial plane, these objects are descending in latitude from north to south, against the flow of the predictable “patterns of life” nominally observed for derelict motion at GEO. This discrepancy in the latitude cycle indicates that the descending nodes of the outliers are currently located near the ascending nodes of the synchronized objects clustered in neighboring longitude slots. This paper is thereby borne out of the quest to characterize the apparent anomalous motion of these eight outlying objects, by studying whether such asynchronicity in latitude can arise under well-known RAAN dynamics at GEO driven by the coupling between luni-solar perturbations and central body oblateness (Chao, 2005).

Specifically, this paper provides a unifying summary of “bottom-up” analytical theory with “top-down” observational data to highlight the common linkage between these two dimensions of GEO debris behavior. The relevance of naturally-occurring patterns of debris motion at GEO to current and future operations in the GEO arena is discussed, and long-term implications of these tendencies to space situational awareness (SSA) in this arena are highlighted.

## 2. Inclination and RAAN variations induced by luni-solar perturbations

The doubly-averaged<sup>2</sup> differential equations of motion governing inclination  $i$  and right ascension of the ascending node  $\Omega$  variations induced by luni-solar perturbations prominent at the GEO altitude are, for near-circular orbits only, given by (Chao, 2005; Chobotov, 2002)

$$\frac{di}{dt} = \sum_{j=1}^2 \frac{3}{8} \gamma_j [\cos(i) \sin(2i_j) \sin(\Omega - \Omega_j) + \sin(i) \sin^2(i_j) \sin(2(\Omega - \Omega_j))] \quad (1)$$

$$\begin{aligned} \frac{d\Omega}{dt} = & -\frac{3}{2} J_2 \left( \frac{R_{\oplus}}{a} \right)^2 n \cos(i) \\ & + \sum_{j=1}^2 \frac{3}{16} \left( \frac{\gamma_j}{\sin(i)} \right) [\sin(2i)(1 - 3 \cos^2(i_j)) \\ & + 2 \cos(2i) \sin(2i_j) \cos(\Omega - \Omega_j) \\ & + \sin(2i) \sin^2(i_j) \cos(2(\Omega - \Omega_j))] \end{aligned} \quad (2)$$

where the summations are performed over the Sun and the Moon, respectively, with  $\gamma_j \equiv n_j^2 R_m / n$  for third-body mass

<sup>2</sup> Termed “doubly” averaged because the complete equations of motion for inclination and RAAN have been averaged once over true anomaly, and a second time over argument of perigee, such that short-period and long-period oscillations in inclination and RAAN have been removed, leaving secular variations only (Chao, 2005).

Download English Version:

<https://daneshyari.com/en/article/1763209>

Download Persian Version:

<https://daneshyari.com/article/1763209>

[Daneshyari.com](https://daneshyari.com)